Title

Cell-mediated remodeling of biomimetic encapsulating hydrogels triggered by adipogenic differentiation of adipose stem cells.

Authors

Clevenger, Tracy N
Luna, Gabriel
Boctor, Daniel
et al.

Publication Date

2016

DOI

10.1177/2041731416670482

Peer reviewed

Original Article

Journal of Tissue Engineering
Volume 7: 1–12

DOI: 10.1177/2041731416670482
tej.sagepub.com
SAGE

Cell-mediated remodeling of biomimetic encapsulating hydrogels triggered by adipogenic differentiation of adipose stem cells

Tracy N Clevenger[1,2,3], Gabriel Luna[2,4], Daniel Boctor[2], Steven K Fisher[2,4] and Dennis O Clegg[1,2,3]

Abstract

One of the most common regenerative therapies is autologous fat grafting, which frequently suffers from unexpected volume loss. One approach is to deliver adipose stem cells encapsulated in the engineered hydrogels supportive of cell survival, differentiation, and integration after transplant. We describe an encapsulating, biomimetic poly(ethylene)-glycol hydrogel, with embedded peptides for attachment and biodegradation. Poly(ethylene)-glycol hydrogels containing an Arg–Gly–Asp attachment sequence and a matrix metalloprotease 3/10 cleavage site supported adipose stem cell survival and showed remodeling initiated by adipogenic differentiation. Arg–Gly–Asp–matrix metalloprotease 3/10 cleavage site hydrogels showed an increased number and area of lacunae or holes after adipose stem cell differentiation. Image analysis of adipose stem cells in Arg–Gly–Asp–matrix metalloprotease 3/10 cleavage site hydrogels showed larger Voronoi domains, while cell density remained unchanged. The differentiated adipocytes residing within these newly remodeled spaces express proteins and messenger RNAs indicative of adipocytic differentiation. These engineered scaffolds may provide niches for stem cell differentiation and could prove useful in soft tissue regeneration.

Keywords

Adipose stem cells, regenerative medicine, MMP3, Arg–Gly–Asp, poly(ethylene)-glycol hydrogel, biodegradable, biomimetic

Received: 21 July 2016; accepted: 31 August 2016

Introduction

The development of biocompatible materials has advanced the field of tissue engineering by providing novel cellular platforms for the promotion of tissue regrowth.[1] Many fields in regenerative medicine including the treatment of chronic wounds stand to benefit significantly from advances in biomaterial engineering. It is estimated that 1%–2% of people in the developed countries will experience a chronic wound in their lifetime, and that in the United States alone 6.5 million patients suffer from chronic wounds.[2,3] Additionally, soft tissue injuries constitute a large portion of blast-related wounds experienced by active military personnel, and because of their extensive

[1]Center for Stem Cell Biology and Engineering, University of California, Santa Barbara, CA, USA
[2]Neuroscience Research Institute, University of California, Santa Barbara, CA, USA
[3]Department of Molecular, Cellular, and Developmental Biology, University of California, Santa Barbara, CA, USA
[4]Center for Bio-Image Informatics, University of California, Santa Barbara, CA, USA

Corresponding author:
Dennis O Clegg, Center for Stem Cell Biology and Engineering, Neuroscience Research Institute, University of California, Santa Barbara, CA 93106-5060, USA.
Email: dennis.clegg@lifesci.ucsb.edu

variability and complexity, they are not amenable to standard treatments.[4,5]

Interest in the use of human adipose stem cells (ASCs) as a potential method to treat traumatic or blunt-force injuries has steadily grown over the last decade. Adipose-derived stem cells are a multipotent stem cell population found in abundance in adult humans, and they possess attributes well-suited for regenerative applications. Autologous ASCs are easily obtained through standard liposuction procedures and can be expanded in culture. They have immunomodulatory properties and secrete vital growth factors, such as vascular endothelial growth factor (VEGF), which is an important molecule involved in the wound healing process.[6] Recently, it was demonstrated that the addition of ASCs to a chronic wound site decreased healing times, and that seeding ASCs on the surface of synthetic membranes showed an even greater benefit, increasing healing by 50%.[7,8]

Biomimetic frameworks that provide structural support and signaling cues derived from the extracellular matrix (ECM) may aid survival of transplanted cells. Poly(ethylene)-glycol (PEG), a water-soluble polymer, is currently used to extend the duration of interferon-alpha in humans as treatment for hepatitis C and can aid in the stimulation of neutrophil production in neutropenia.[9,10] The hydrogels manufactured from this polymer can be functionalized to provide cell attachment and degradation sites and may also be adapted for use in drug delivery systems and as substrates for cell transplantation.[11–13] The chemical versatility of PEG allows for the incorporation and modification of components that create a synthetic ECM closely mimicking an environment that, at the molecular level, can specifically interact with a given cell type in a directed manner.[14–16]

One approach to encapsulation involves using thiol-functionalized multi-arm PEG groups that use divinyl sulfone (DVS) as a crosslinker to polymerize the hydrogels through a Michael-type addition chemical reaction. This method avoids the need for a catalyst that has the potentially detrimental effect on encapsulated cells.[17,18] Furthermore, these PEG-based hydrogels possess the ability to incorporate peptides through thiol chemistry using a free cysteine. Peptides containing Arg–Gly–Asp (RGD) sequences can serve as attachment sites for cells, via integrin binding, in the inert PEG gel.[19] Sequences containing RGD have been shown to induce fibroblast spreading,[20] maintain embryonic stem cells,[21] influence mineralization by osteogenic cells,[22] promote the migration of smooth muscle cells through the hydrogels,[23] and regulate differentiation of various cell lines, such as endothelial cells and myoblasts.[24–27] Modulation of the RGD-containing sequence can influence survival, proliferation, and differentiation, indicating that synthetic environments can be engineered to generate specific cell populations with specific functions.[18]

In this study, we describe efforts to develop an encapsulating hydrogel for ASC that will remodel upon differentiation of ASCs to adipocytes. As a result of elevated levels of MMP3 and MMP10 (two members of the stromelysin family of MMPs) produced by adipocytes,[28,29] a scaffolding system was developed that used an MMP peptide cleavage site specific to MMPs 3/10 (GR**C**GRPKPQQ↓FFGLMG; hereafter MMPc).[30,31] We characterized ASCs encapsulated in this hydrogel in vitro and show accelerated generation of lacunae within the gel after differentiation.

Materials and methods

Cell culture

ASCs were isolated from donated lipoaspirate and purified using methods previously described elsewhere.[18,32–34] Briefly, lipoaspirate was washed 5–10 times using phosphate buffered saline (PBS; pH 7.4) containing 1× penicillin–streptomycin. Next, the lipoaspirate was digested using 0.15% collagenase type I solution (220.00 units/mg; Thermo Fisher, Carlsbad, CA, USA). The cell solution was then pelleted by centrifugation at 1000×*g* for 10 min and resuspended in a solution containing 160 mM ammonium chloride. Cells were then recentrifuged and resuspended in media containing 60% Dulbecco's modified Eagle's medium (DMEM; Thermo Fisher, Carlsbad, CA, USA) with 10% fetal bovine serum (FBS) and 40% MesenPro medium (Thermo Fisher, Carlsbad, CA, USA). Finally, the cells were characterized using flow cytometry. Cultures were determined to be CD73-, CD90-, and CD105-positive, as well as CD45- and CD31-negative, consistent with the ASC immunophenotype defined by the guidelines set forth by the International Federation for Adipose Therapeutics and Science (IFATS) and the International Society for Cellular Therapy (ISCT).[35]

Cells at passages 2–4 were harvested from tissue culture flasks and encapsulated at 10×10^6 cells/mL in a 10-kDa PEG hydrogel (PEGworks, Chapel Hill, NC, USA) prior to polymerization. They were then crosslinked using DVS (Sigma–Aldrich, St Louis, MO, USA; PEG–DVS) as described previously.[18] A biotin-tagged RGD-containing peptide (VnRGD; CGRCGKGGPQVT**RGD**VFTMPG-K(biotin)) derived from the full-length vitronectin amino acid sequence was incorporated to provide attachment sites for the undifferentiated ASCs. In a subset of experiments, a peptide was incorporated that contained a site for cleavage by MMP3/10 (ac-GR**C**GRPKPQQ↓FFGLMG-NH_2), derived from the sequence found in Substance P, a known substrate.[30] Cells were cultured in three-dimensional (3D) hydrogels in either MesenPro or adipogenic differentiation media for 24 h or 4 weeks.[18] Adipogenic differentiation medium consisted of alpha-modified minimum essential medium (Sigma–Aldrich, St. Louis, MO, USA), supplemented with 10% FBS (Atlas Biologicals, Fort Collins,

Table 1. TaqMan probes used for gene expression analysis.

Gene	Gene Name	Assay ID	Marker cell type
PPARG	Peroxisome proliferator–activated receptor gamma	Hs00234592_m1	Adipocyte
ADIPOQ	Adiponectin	Hs00605917_m1	Adipocyte
ACAN	Aggrecan	Hs00153936_m1	Chondrocyte
ALPL	Alkaline phosphatase	Hs01029144_m1	Osteocyte
vWF	von Willebrand factor	Hs01109446_m1	Endothelial
MMP3	Matrix metallopeptidase 3 (stromelysin 1)	Hs00968305_m1	–
GAPDH	Glyceraldehyde-3-phosphate dehydrogenase	Hs02758991_g1	Housekeeper
ACTB	Actin, beta	Hs01060665_g1	Housekeeper
UBC	Ubiquitin C	Hs01871556_s1	Housekeeper
GPI	Glucose-6-phosphate isomerase	Hs00976715_m1	Housekeeper

CO, USA), 2 mM L-glutamine (Life Technologies), 100 mM indomethacin (Sigma–Aldrich), 10 mg/mL insulin (Sigma–Aldrich), 1 mM dexamethasone (Sigma-Aldrich), 500 mM 3-isobutyl-1-methylxanthine (Sigma–Aldrich), and 10 U/mL penicillin–streptomycin (Life Technologies, Carlsbad, CA, USA).

Enzyme-linked immunosorbent assay

In order to examine the amounts of cleaved biotin, an enzyme-linked immunosorbent assay (ELISA) was performed. Here, ASCs were encapsulated into PEG–DVS hydrogels with VnRGD, in the presence of the MMPc cleavage peptide. The hydrogels were grown in either adipogenic culture media or MesenPro media; media were then harvested 24 h after polymerization and at 4 weeks. Samples used to analyze 4-week time points were harvested from media that were added 72 h prior to the time point. Samples were diluted 1:2000, and the amount of biotin released into the media was determined using a Vitamin H ELISA kit (MDBioscience, St Paul, MD, USA; Cat# M046019).

Quantitative real-time polymerase chain reaction

After 4 weeks of culture, gels containing MMPc peptides were frozen in liquid nitrogen and manually homogenized in 1 mL of TRIzol (Thermo Fisher, Carlsbad, CA, USA) containing 5 µg/mL *Saccharomyces cerevisiae* tRNA (Sigma–Aldrich; Cat# R8508) for 3 min.[36] Next, 100 µL of chloroform was added and samples were centrifuged at 15,000 r/min for 18 min at 4°C. The aqueous phase was removed and recentrifuged at 15,000 r/min for 10 min at 4°C. The aqueous phase was then removed and an equal volume of 100% EtOH was added. The resultant solution was then added to RNeasy MinElute spin columns and subsequent steps were followed in accordance with the RNeasy MinElute Cleanup kit protocol (Qiagen, Hilden, Germany; Cat# 74204). RNA was used for complementary DNA (cDNA) synthesis using an iScript cDNA synthesis kit (BioRad, Hercules, CA, USA; Cat# 1708891). Predesigned TaqMan (Thermo Fisher, Canoga Park, CA, USA) probes used to examine gene expression are shown in Table 1.

Preparation and immunocytochemistry

After 24 h or 4 weeks in culture, samples were washed 3× for 5 min in PBS and then immersion fixed in 4% paraformaldehyde in 0.1 M sodium cacodylate (Electron Microscopy Sciences, Hatfield, PA, USA) for 30 min at room temperature. Samples were then cryo-protected using a gradient series of 10%, 20%, and 30% sucrose in PBS for 2 h each and placed in 40% sucrose overnight at 4°C. The following day, samples were immersed in optimal cutting temperature (OCT) media (Electron Microscopy Sciences) on a rotator overnight at room temperature. Finally, samples were embedded in OCT media, frozen using liquid nitrogen, and sectioned at 20 µm.

To identify the hydrogel, slides were immunostained using a streptavidin secondary antibody conjugated to 488 or 568 flurophore (1:100; Jackson ImmunoResearch, West Grove, PA, USA). In order to further characterize developing ASCs, sections were stained using anti-PPAR gamma (PPARG; 1:50; Santa Cruz Biotechnology, Santa Cruz, CA, USA; Cat# sc-271392), anti-MMP3 (1:50; EMD Millipore, Temecula, CA, USA; MAB3306), anti-MAP2 (1:100; EMD Millipore), and Hoechst 33342 (1:5000; Thermo Fisher, Canoga Park, CA, USA) for 1 h at room temperature in PBS containing 0.5% Triton X-100 and 1% bovine serum albumin (BSA) (PBT). Samples were then rinsed 2× for 5 min in PBT and subsequently mounted using Prolong Gold (Invitrogen, Carlsbad, CA, USA) under a glass cover slip.

Mosaic acquisition and image registration

Digital micrographs were captured using an Olympus Fluoview 1000 laser scanning confocal microscope (Olympus America Inc., Center Valley, PA, USA) equipped with a precision automated motorized stage (Applied Scientific Instrumentation Inc., Eugene, OR, USA), using

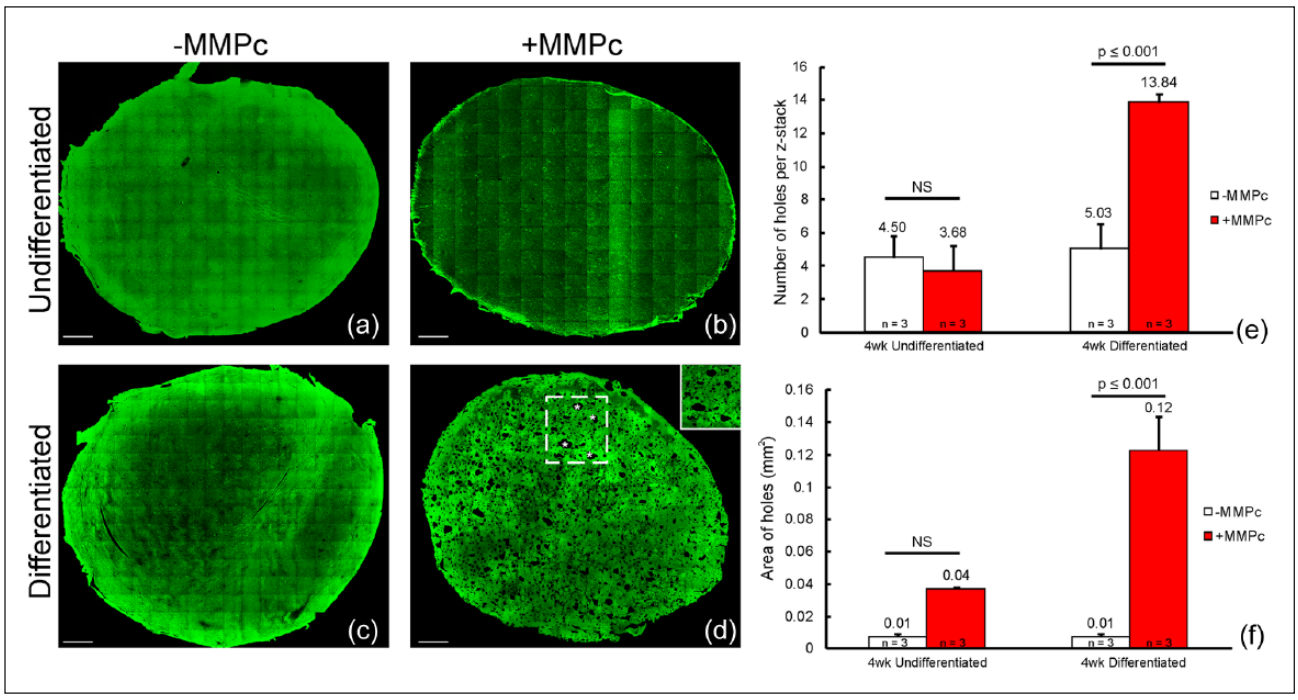

Figure 1. Remodeling of MMPc-containing hydrogels after ASC differentiation. Gel architecture was assessed via staining for biotin (green), which was present in the covalently attached RGD peptide. Gels cultured with undifferentiated ASC for 4 weeks (a) without and (b) with MMPc peptide showed few holes. Likewise, gels cultured with differentiated ASC, (c) without MMPc peptide showed fewer, smaller holes. However, gels cultured with differentiated ASC, (d) with MMPc peptide showed an increased number and area of holes. (e) The number of holes quantified. (f) The area of holes quantified. Scale bars = 500 µm.

either an UPlanFLN 40× (N.A. 1.30) or an UPlanSApo 20× (N.A. 0.75) lens. Datasets were collected as individual z-stacks captured at a pixel array of either 1024 × 1024 or 800 × 800. Optical sections were collected at 1-µm intervals with a 5% overlap along the *x*- and *y*-axes; finally, resultant datasets were automatically maximally projected, aligned, and registered using Imago 1.5 (Mayachitra Inc., Santa Barbara, CA, USA) to yield wide-field high-resolution mosaics of the sectioned 3D hydrogels in a manner previously described.[37] All datasets used for spatial analyses have been deposited to Bisque (Bio-Image Semantic Query User Environment) and are publically available for further interrogation with permission (http://bisque.ece.ucsb.edu/client_service/view?resource=http://bisque.ece.ucsb.edu/data_service/00-BCLMKCcAJrQ2XHUpXx4fnf).[38]

Image analysis

Images were analyzed using open source ImageJ software (National Institutes of Health, Bethesda, MD, USA) to quantify both the number and size of the holes present in each mosaic. Each z-stack was first projected as a two-dimensional (2D) image, and subsequently a threshold for detection of fluorescence was applied across all images analyzed. Images were then converted to a binary format and analyzed for particles using a set size (140–7000) and a circularity of (0.37–1) to ensure that only the holes were included while the edge artifacts were excluded from quantitative analyses. Here, statistical significance was defined as $p \leqslant 0.05$ using a one-tailed Student's *t*-test.

Results

In a previous study, we described a simple, encapsulating RGD peptide hydrogel that supported survival and differentiation of ASCs. In this study, we sought to develop a hydrogel that will be remodeled during differentiation to provide spaces to accommodate adipocytes. Due to adipocytes producing elevated levels of MMP3 and MMP10,[28,29] we incorporated peptides containing MMP cleavage sites recognized by these enzymes. The most promising peptide (GR**C**GRPKPQQ↓FFGLMG; hereafter MMPc) was selected for further study.[30,31]

After 4 weeks in maintenance media (MesenPro), 3D synthetic scaffolds with and without MMPc peptide showed no structural changes (Figure 1(a) and (b); green). Similarly, scaffolds that did not contain MMPc and cultured in adipogenic differentiation media for 4 weeks displayed no structural changes (Figure 1(c)). However, the inclusion of MMPc resulted in significant structural changes in the gels after 4 weeks of adipogenic differentiation with an increased number of holes observed (Figure 1(d); green; asterisk, inset). After 4 weeks, no

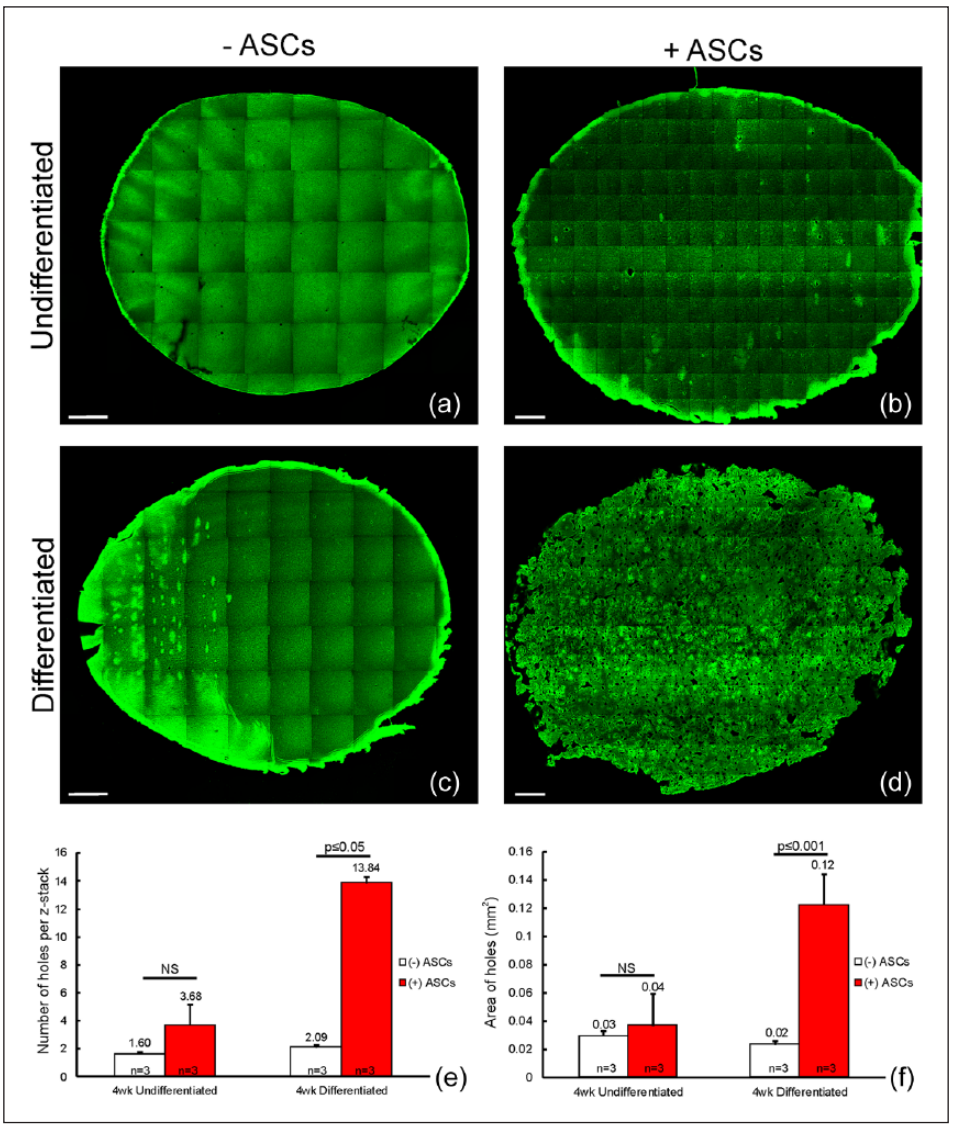

Figure 2. Remodeling is dependent on the differentiation of ASC in MMPc-containing hydrogels. Gel architecture was assessed via staining for biotin (green), which was present in the covalently attached RGD peptide. Gels cultured 4 weeks in the absence of ASC, (a) under undifferentiated culture conditions or (c) in differentiation media showed fewer and smaller holes. Gels cultured 4 weeks in the presence of ASC, (b) under undifferentiated culture conditions likewise showed fewer, smaller holes. However, gels cultured 4 weeks in the presence of ASC, (d) in differentiation media showed an increased number and area of holes. (e) The number of holes quantified. (f) The area of holes quantified. Scale bars = 500 µm.

statistical significance in the average number of holes was observed between the undifferentiated samples with and without MMPc. However, after 4 weeks of differentiation, there was a statistical significance in the average number of holes per z-stack between the hydrogels that contained the cleavage peptide (13.84 holes/z-stack) and those that did not (5.03 holes/z-stack; Figure 1(e); $p \leqslant 0.001$). Additionally, no statistical significance in the average area of holes per z-stack was observed between the undifferentiated hydrogel with (0.04 mm^2) and without (0.01 mm^2) the cleavage peptide. The average area of holes in the differentiated hydrogels with MMPc was significantly increased compared to the differentiated gels without MMPc as well as both the undifferentiated conditions (Figure 1(f); $p \leqslant 0.001$).

To determine whether the ASCs were responsible for the generation of the holes in the MMPc scaffolds, the hydrogels were cultured for 4 weeks with and without the undifferentiated ASCs and no structural changes were observed in the number or sizes of the holes (Figure 2(a) and (b); green). The hydrogels containing MMPc that were differentiated for 4 weeks in the absence of ASCs also appeared structurally similar to those in the undifferentiated conditions (Figure 2(c); green). However, scaffolds containing the differentiated ASCs in the presence of MMPc showed a markedly increased number of holes (Figure 2(d)).

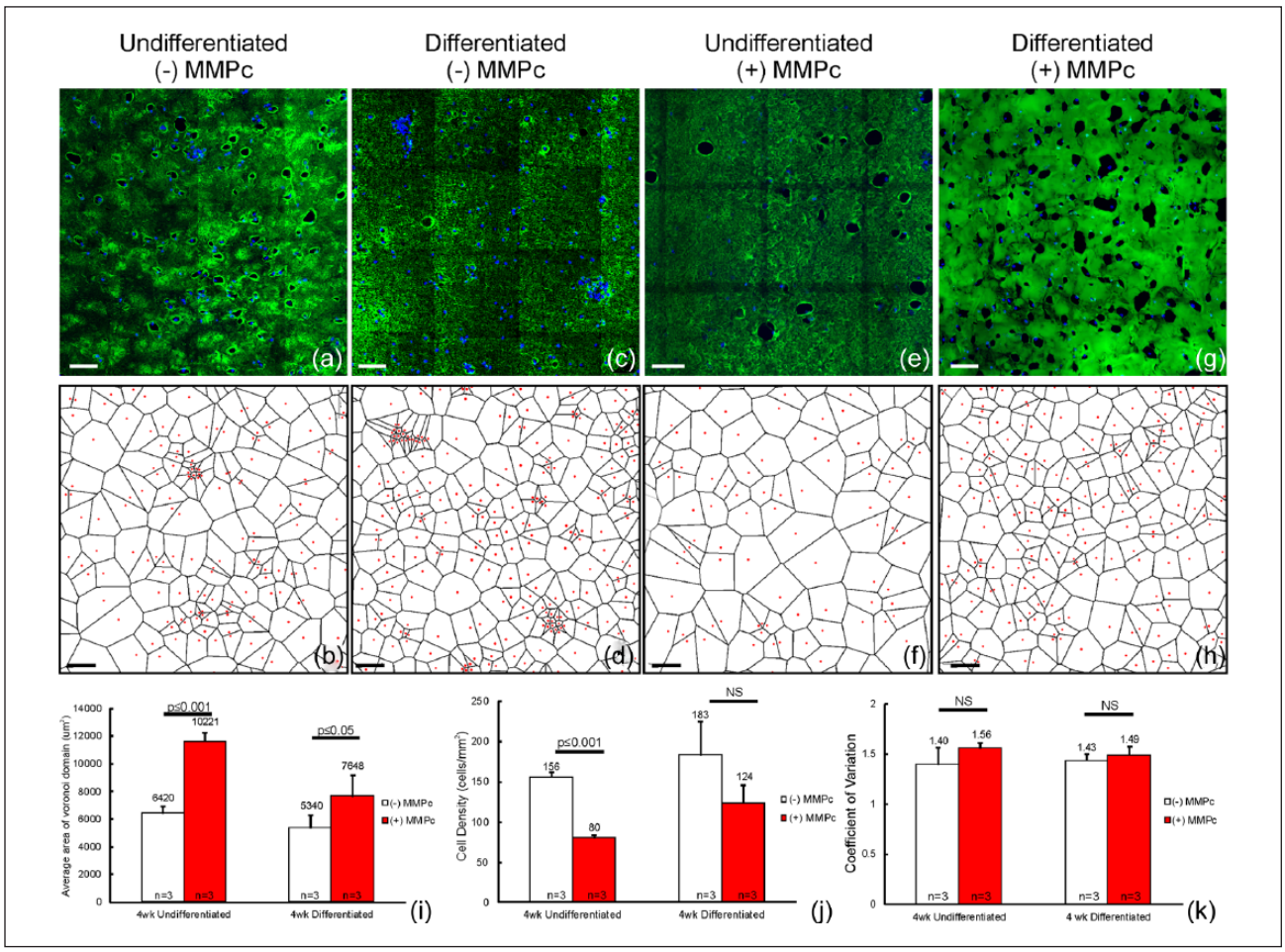

Figure 3. Average Voronoi areas. Gel architecture was assessed via staining for biotin (green), which was present in the covalently attached RGD peptide. Micrographs shown represent hydrogels cultured for 4 weeks (a and c) without MMPc and (e and g) with MMPc in undifferentiated and differentiated conditions. Representative images of Voronoi domains are shown in b, d, f, and h. (i) Quantification of the average Voronoi areas. (j) Quantification of cell densities in all conditions. (k) Distribution of cells was determined to display a random appearance determined by employing the coefficient of variation analysis. Scale bars = 100 µm.

Indeed, subsequent quantification showed no statistical significant difference in the number of holes per z-stack in the hydrogels that were cultured in maintenance media with or without ASCs. In contrast, gels that were differentiated in the presence of MMPc with ASCs showed a greater than 6-fold increase in the number of holes per z-stack compared to those without ASCs (Figure 2(e); $p \leqslant 0.001$). Similarly, the area of holes between the undifferentiated conditions (i.e. with and without ASCs) showed no statistical significant difference (0.03 vs 0.04 mm^2). The area of holes in the differentiated gels containing MMPc peptide in the presence of ASCs showed a distinct increase (Figure 2(f); 0.12 vs. 0.02 mm^2; $p \leqslant 0.001$).

Voronoi domains were used to describe the 2D spatial organization of the ASCs across experimental conditions. Manual annotations of Hoechst-stained nuclei were used and the Cartesian x–y coordinates on these nuclei were recorded in the hydrogels cultured for 4 weeks (Figure 3(a), (c), (e), and (g)). Voronoi domain diagrams were generated and their respective areas computed (Figure 3(b), (d), (f), and (h)). In the undifferentiated conditions, Voronoi domain area averaged 6420 μm^2. By comparison, the hydrogels containing the MMPc peptide showed a statistically significant increase in the average area of Voronoi domains (10,221 μm^2, $p \leqslant 0.001$; Figure 3(i)). Likewise, samples cultured in differentiation media also showed a statistically significant increase in the average Voronoi domain area between gels without MMPc (5340 μm^2) and those with MMPc (7648 μm^2; $p \leqslant 0.05$). To further support the changes observed in the average area of Voronoi domains in the undifferentiated conditions, cell densities were computed, and it was determined that in samples not containing MMPc there was a statistically significant increase in the density of cells (156 cells/mm^2) compared to those gels with MMPc (80 cells/mm^2; $p \leqslant 0.001$). In contrast, samples cultured in differentiation media showed no statistical difference in cell density (124 cells/mm^2; +MMPc and 183 cells/mm^2;

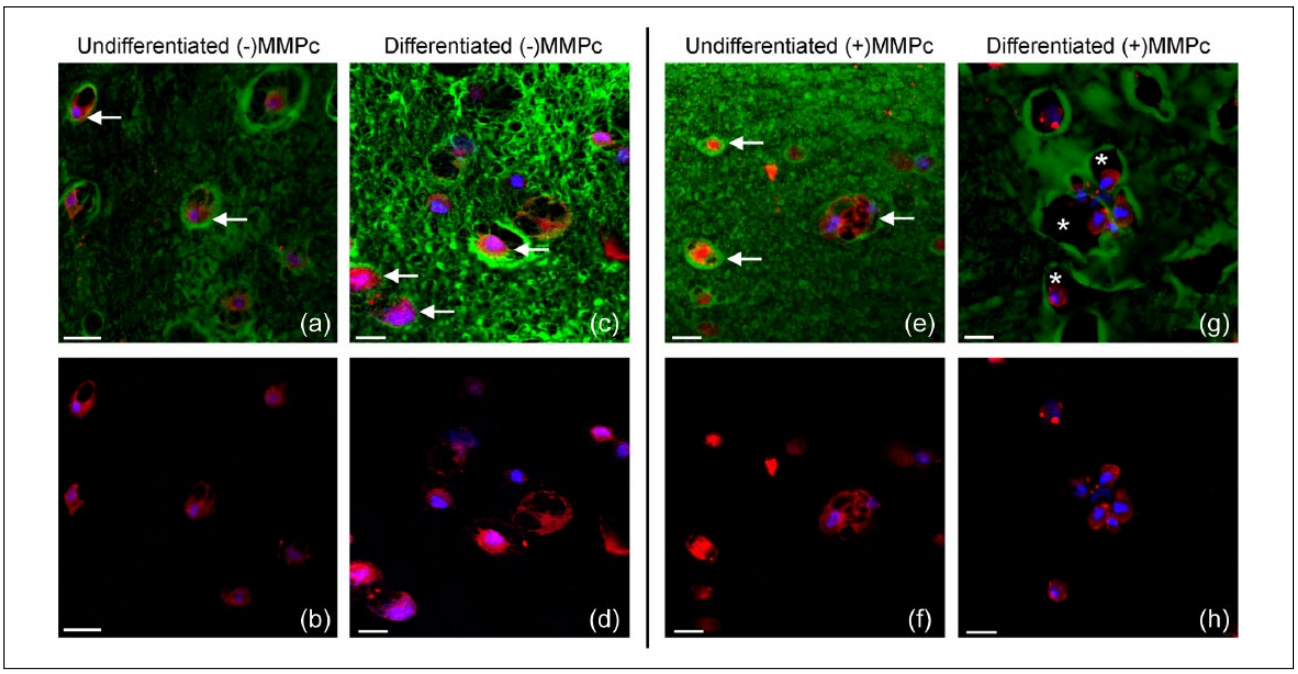

Figure 4. Cell morphology in hydrogels ± MMPc. Micrographs of hydrogels cultured for 4 weeks (a–d) without and (e–h) with MMPc, in undifferentiated and differentiated conditions are shown. Arrows indicate protrusions of the cellular membrane. Asterisks indicate holes formed in the +MMPc differentiated condition. Green: biotin; red: Map 2; blue: Hoechst. Scale bars: 20 µm.

−MMPc; Figure 3(j)). Finally, a coefficient of variance analysis (i.e. standard deviation/mean of the Voronoi domains) was performed to determine whether there was cell clustering observed in any condition. It was determined that no condition demonstrated an increased clustering of cells in 2D (Figure 3(k)).

Encapsulated cells were further analyzed using immunocytochemistry. Cells appeared adjacent to the peripheral margins of the holes in the hydrogel (Figure 4(a), (c), and (e); arrows). Similarly, ASCs that were differentiated for 4 weeks in samples with MMPc remained positioned near the edges of the holes in the remodeled gel, although they never increased in size to occupy vacant spaces caused by the remodeling process of the PEG gel (Figure 4(g); asterisks). Under these conditions, the gel displayed an increased level of fluorescent intensity at the boundary of the holes, as indicated by biotin staining (green). To rule out trapping of streptavidin, sections were stained with hemotoxylin and eosin, which revealed increased labeling at the boundary of the holes (Supplemental Figure 1). Additionally, cells in each condition had a rounded appearance, indicated by anti-MAP2 staining, a hallmark morphological appearance of adipocytes (Figure 4(b), (d), (f), and (h); red).[39]

Adipose-derived stem cells that were undifferentiated in gels with the MMPc cleavage site showed only nonspecific anti-PPARG labeling compared to the elevated labeling observed in ASCs that had been differentiated for 4 weeks (Figure 5(a)–(d)). Anti-PPARG labeling appeared to display perinuclear localization in ASCs under the differentiated conditions (Figure 5(d); arrows). Additionally, immunolabeling for the MMP3/10 protein was also increased in the differentiated state (Figure 5(e)–h). In the differentiated state, a majority of the ASCs were MMP 3/10 immunopositive (Figure 5(h); arrows). Gene analysis determined a statistically significant increase in two adipogenic genes (PPARG and *ADIPOQ*) in the differentiated samples. Chondrogenic and endothelial genes examined (*ACAN* and *vWF*, respectively) showed no expression in either the differentiated or undifferentiated conditions. Expression of MMP3 showed an increase in samples that were adipogenically differentiated compared to the undifferentiated counterparts (Figure 5(i)).

Finally, to investigate degradation of the system, biotin levels were quantified as they were released into the media after adipocytic differentiation. Biotin is attached to the RGD peptide, which was covalently attached to the PEG backbone. A significant increase in the amount of biotin was detected at 4 weeks in gels with the differentiated ASCs (1822.60 ng/mL), compared to the undifferentiated samples (1678.70 ng/mL; Figure 5(j)).

Discussion

Previous work has demonstrated that the PEG–DVS hydrogel system allows for the survival and differentiation of ASCs into mature adipocytes.[18] These PEG-based scaffolds have demonstrated robust biostability in culture, showing no significant degradation over a 1-month period. However, the ASCs were constrained in close proximity to the surrounding gel, which may not allow for diffusion

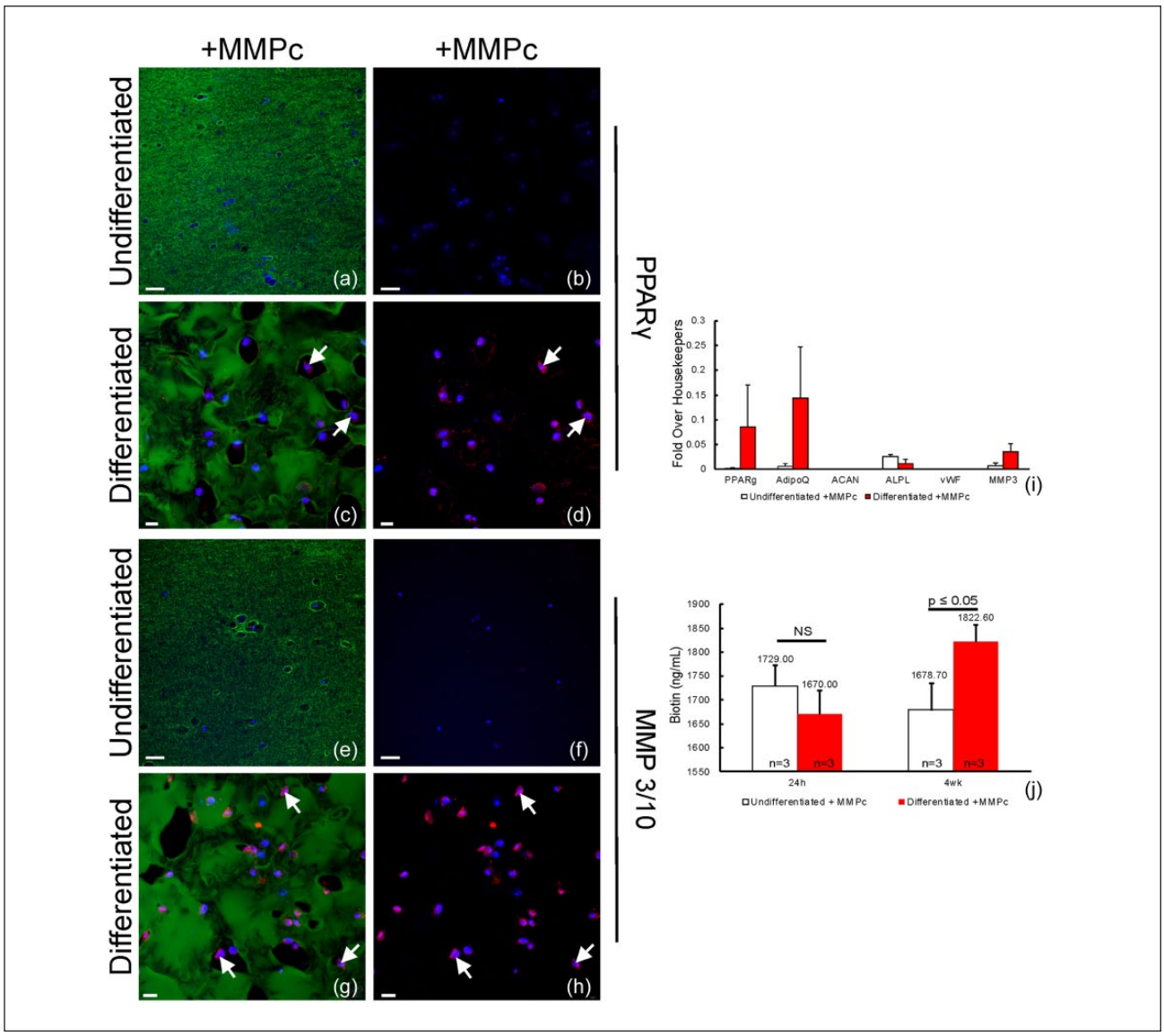

Figure 5. Expression of PPARγ and MMP3/10 in MMPc-containing hydrogels. (a and b) No expression of PPARγ was detected after 4 weeks of culture in undifferentiated conditions, (c and d—arrows) but expression was observed after 4 weeks of adipogenic differentiation. Likewise, (e and f) no expression of MMP3/10 was detected after 4 weeks of culture in undifferentiated conditions, (g and h—arrows) but expression was observed after 4 weeks of adipogenic differentiation. (i) Quantification of mRNAs showed an increase in adipogenic markers (PPARγ, AdipoQ) in differentiated cultures, but not in chondrogenic (ACAN), osteogenic (ALPL), or endothelial (VWF) markers and also showed an increase in MMP3 expression. (j) Release of biotin into the media during culture. Green: biotin; red: PPARγ or MMP3/10; blue: Hoechst. Scale bars: a, b, e, f = 50 µm; c, d, g, h = 20 µm.

of secreted ECM, optimal differentiation, or investiture of the vasculature after transplant. Therefore, we sought to modify the hydrogel to allow remodeling upon differentiation to generate spaces to accommodate adipose cells. Research has shown that incorporated peptide crosslinks are susceptible to enzymatic degradation by MMPs.[17,40–44] These previous approaches often utilize a peptide that includes two cysteine residues flanking an MMP cleavage site for common MMP collagenases, allowing for generic degradation. Collagenases comprise the largest known class of MMPs, and by utilizing these cleavage sites, degradation of the hydrogel can be very rapid.

Here, a novel MMP peptide was incorporated containing the cleavage site recognized by MMP3 and MMP10, which are known to be elevated in adipocytes. Surprisingly, it was determined that a peptide containing only a single cysteine residue (MMPc) permitted remodeling as encapsulated ASCs differentiate into mature adipocytes. Data presented here show that these functionalized scaffolds contained an increased number and size of lacunae after differentiating the ASCs for 4 weeks in culture, a phenomenon not seen in samples with the undifferentiated ASCs. Here, we report the first use of a monocysteine MMP peptide to provide a site for degradation of a synthetic scaffold. Furthermore, the

remodeling occurred only in the presence of the differentiated ASCs, indicating that it is unlikely a result of a breakdown of the hydrogel over time or an artifact of long-term culture alone. Additionally, this novel demonstration of remodeling is initiated by adipogenic differentiation in a PEG-based hydrogel. The density of cells per square millimeter in the differentiated conditions containing the MMPc showed no statistically significant change between 24 h and 4-week time points, thus indicating the cells remain viable for the duration of these studies.

Voronoi domains quantitatively reveal the distribution of ASCs in 2D space across experimental conditions; additionally, it demonstrated that the incorporation of the MMPc site is correlated with the presence of larger Voronoi areas signifying that the cellular distribution in these degradable scaffolds varied from their counterparts. However, cell density in the differentiated conditions was not significantly altered by the inclusion of an MMPc site, indicating that the increase in area of Voronoi domains was not a result of a reduction in the number of ASCs present after 4 weeks of culture. Interestingly, the differentiation of these cells elicited an increase in density not observed in the undifferentiated samples ($p \leqslant 0.01$). The increase in density may be indicative of increased cell viability due to the deposition of ECM by the differentiating cells in the presence of increasing number of holes, a process that may be absent in the undifferentiated cultures. In the differentiated conditions, the increase in Voronoi domain area of the MMPc-containing samples reflects a more even cellular distribution across the hydrogel. There appears to be more instances of cell clustering in the differentiated samples without MMPc. It is plausible that the increase in the number of holes provides an environment that is more conducive to cell mobility. Finally, a coefficient of variation analysis was used to determine the relative distribution of ASCs throughout each condition revealing that no condition exhibited a unique distribution of cells (i.e., clustering). A homogeneous distribution of ASCs in a scaffolding system may be important in improving therapeutic approaches to tissue regeneration.

General cellular morphology was examined by probing for the cytoskeletal marker MAP2. Anti-MAP2 labeling revealed that ASCs in an undifferentiated state in both the presence and absence of MMPc showed protrusions representing potential attachment sites to the hydrogel. These extensions were also noted in the differentiated samples without MMPc although to a lesser extent. However, the hydrogels containing the MMPc site with the differentiated ASCs displayed no visible protrusions emanating from ASCs. Cells in this condition showed a more rounded morphology, congruent with the typical phenotype of adipogenic cell differentiation.[39]

Adipogenic differentiation of the ASCs in MMPc gels was confirmed by the immunocytochemical presence of the nuclear receptor PPARG. At the transcriptional level, adipogenic differentiation of ASCs was examined via real-time quantitative polymerase chain reaction (RT-qPCR). Two genes commonly used to characterized adipose tissue are *PPARG* and *ADIPOQ*; here, it was observed that both increased in the differentiated samples. Since adipogenic differentiation has previously been examined in these PEG gels without MMPc[18], here efforts were placed on examining the differentiation in MMPc-containing hydrogels.

Gene expression analysis for contaminating cell types was also examined in the differentiated samples, although no detectable levels of chondrogenic (*ACAN*) or endothelial cell (*vWF*) genes were observed, as well as no significant changes in an osteogenic (*ALPL*) gene. Increased expression of MMP3 was confirmed at both the gene and protein levels in the differentiated condition and was not detected in the undifferentiated condition. The increase in MMP3/10 expression (both protein and gene) supports the hypothesis that as ASCs in the hydrogels continue to differentiate into mature adipocytes, they increase their expression of MMP3/10.

The data presented here lead to the hypothesis that the degradation peptide covalently attaches to the polymer via the cysteine residue near the C-terminus. While the N-terminus does not covalently attach to the network, it is able to crosslink the polymer via the hydrophobic N-terminal amino acids (FFGLMG; Figure 6). Cleavage of the MMP site by secreted MMP 3/10 is proposed to alleviate these crosslinks and release arms of PEG, thus allowing remodeling of the gel. Increased fluorescent intensity in areas of gel was observed at the edges of the holes, where the polymer may have been redistributed. Portions of gel fragments may also be released, as an increase in biotin (associated with the covalently attached RGD peptide) was detected in the culture media of gels with holes.

By altering various aspects of the system, such as the concentration of MMPc or cell density at time of encapsulation, this scaffold can potentially be modified to remodel and/or degrade in a time- or cell-dependent manner that is appropriate for the target tissue, ranging from weeks to several months. The holes generated by the differentiating cells may also provide a supportive matrix that is tailored by the cells to be specific for an environment accommodating to newly developing tissue. The generation of holes by the differentiated adipocytes not only provides a supportive niche but could aid in angiogenesis of the gel after implantation. The typically poor engraftment and survival of cells in standard fat grafting procedures may benefit greatly from the unique characteristics of this hydrogel system. The increase in the holes as cells differentiate provides an environment, which may be more amenable to vascularization, one of the primary difficulties in the current therapies. The endothelial potential of the transplanted ASCs provides a cell source within the graft to potentially promote vascular incorporation. It has been demonstrated that the inclusion of endothelial progenitor cells promotes graft vascularization and survival.[45] The holes may also provide space necessary for neovascularization. Examinations of preliminary data suggest that the hydrogels without the degradation peptide begin to degrade at approximately 3 months in vivo. Furthermore, based on the relationship in

degradation times in vitro, it is plausible that degradation of the hydrogels with MMPc incorporated will likely show partial degradation as early as 1 month and allow for the rapid incorporation of the transplanted cells.

Novel, encapsulating PEG hydrogels containing an RGD attachment sequence in addition to a matrix metalloprotease 3/10 cleavage site (MMPc) supported ASC survival and showed a regulated remodeling triggered by adipogenic differentiation. These RGD–MMPc hydrogels with encapsulated ASCs showed an increase in the number and area of lacunae or holes upon adipogenic differentiation, providing a niche for the newly developed adipocytes. Tunable, biomimetic hydrogel scaffolds where remodeling of the gel is triggered by adipogenic differentiation may be useful in soft tissue regeneration.

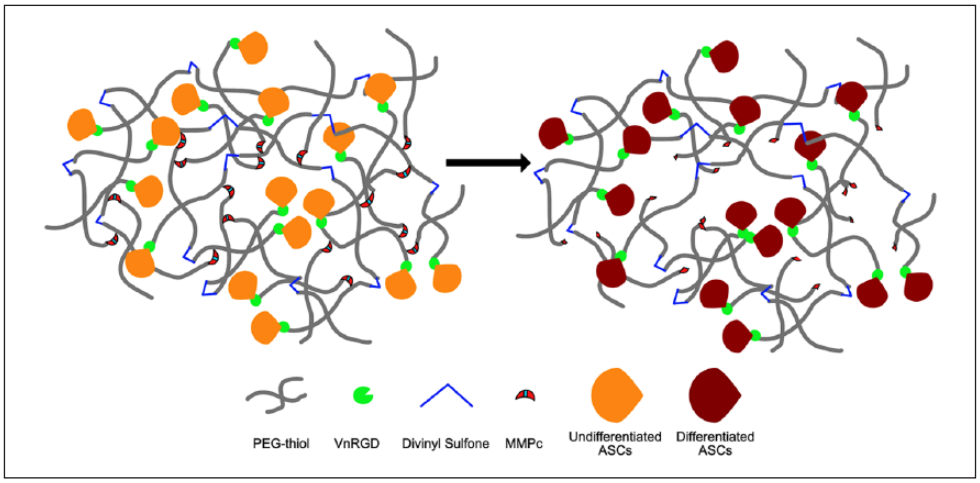

Figure 6. Model of RGD–MMPc hydrogel remodeling upon adipogenic differentiation. The hydrophobic N-terminus of the MMPc peptide may non-covalently interact with the hydrophobic PEG arms. As the ASCs encapsulated in the PEG hydrogel differentiate into adipocytes, they increase the levels of MMP3/10 that are produced. This allows cleavage of the MMPc peptide promoting the remodeling and partial degradation of the scaffolds.

Supplementary information

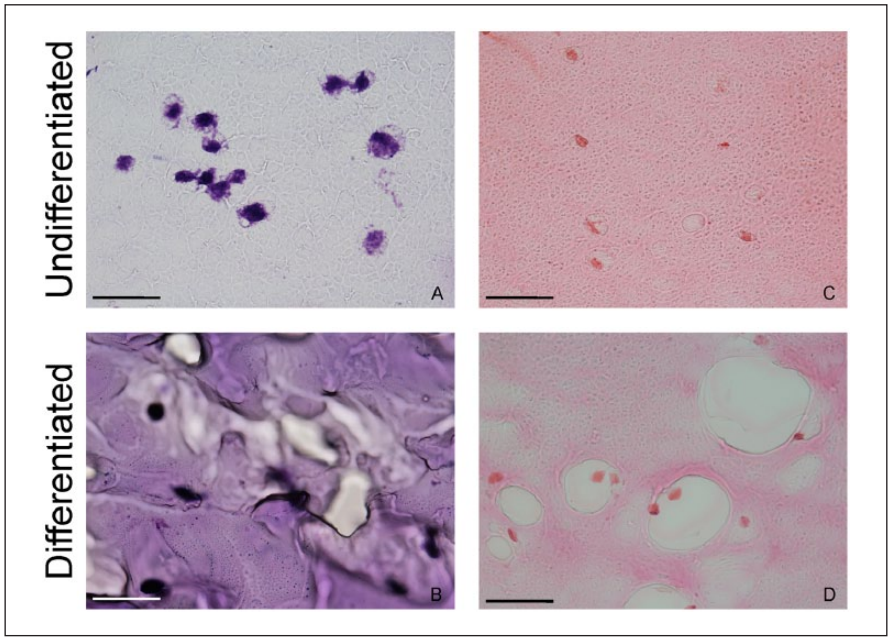

Supplemental Figure 1. Histological stains of MMPc gels. Gels stained with Toluidine Blue show different distributions of nucleic acids present in (a) undifferentiated samples and (b) differentiated samples. Hemotoxylin and eosin staining of (c) undifferentiated and (d) differentiated samples shows altered distribution of hydrogel after adipogenic differentiation.

Declaration of conflicting interests

The content of the information does not necessarily reflect the position or the policy of the Government, and no official endorsement should be inferred. T.N.C. was a predoctoral fellow of the California Institute for Regenerative Medicine.

Funding

D.O.C. was supported by the California Institute for Regenerative Medicine (CIRM; DR1-01444, CL1-00521, TB1-01177, and TG2-01151); CIRM Major Facilities Grant (FA1-00616); and University of California–Santa Barbara, Institute for Collaborative Biotechnologies from the US Army Research Office (W911NF-09-0001). S.K.F. was supported by the National Science Foundation (IIS-0808772 and ITR-0331697).

References

1. Tibbitt MW, Rodell CB, Burdick JA, et al. Progress in material design for biomedical applications. *Proc Natl Acad Sci U S A* 2015; 112(47): 14444–14451.
2. Frykberg RG and Banks J. Challenges in the treatment of chronic wounds. *Adv Wound Care* 2015; 4(9): 560–582.
3. Sen CK, Gordillo GM, Roy S, et al. Human skin wounds: a major and snowballing threat to public health and the economy. *Wound Repair Regen* 2009; 17(6): 763–771.
4. Sheean AJ, Tintle SM and Rhee PC. Soft tissue and wound management of blast injuries. *Curr Rev Musculoskelet Med* 2015; 8(3): 265–271.
5. Santiago GF, Bograd B, Basile PL, et al. Soft tissue injury management with a continuous external tissue expander. *Ann Plast Surg* 2012; 69(4): 418–421.
6. Rehman J. Secretion of angiogenic and antiapoptotic factors by human adipose stromal cells. *Circulation* 2004; 109(10): 1292–1298.
7. Kosaraju R, Rennert RC, Maan ZN, et al. Adipose-derived stem cell-seeded hydrogels increase endogenous progenitor cell recruitment and neovascularization in wounds. *Tissue Eng Part A* 2016; 22(3–4): 295–305.
8. Nie C, Zhang G, Yang D, et al. Targeted delivery of adipose-derived stem cells via acellular dermal matrix enhances wound repair in diabetic rats. *J Tissue Eng Regen Med* 2012; 9(3): 224–235.
9. Arvedson T, O'Kelly J and Yang B-B. Design rationale and development approach for pegfilgrastim as a long-acting granulocyte colony-stimulating factor. *BioDrugs* 2015; 29(3): 185–198.
10. Prabhu RA, Nair S, Pai G, et al. Interventions for dialysis patients with hepatitis C virus (HCV) infection. *Cochrane Database Syst Rev* 2015; 8: CD007003.
11. García AJ. PEG-maleimide hydrogels for protein and cell delivery in regenerative medicine. *Ann Biomed Eng* 2013; 42(2): 312–322.
12. Lin C-C and Anseth KS. PEG hydrogels for the controlled release of biomolecules in regenerative medicine. *Pharm Res* 2008; 26(3): 631–643.
13. Briquez PS, Hubbell JA and Martino MM. Extracellular matrix-inspired growth factor delivery systems for skin wound healing. *Adv Wound Care* 2015; 4(8): 479–489.
14. Kyburz KA and Anseth KS. Synthetic mimics of the extracellular matrix: how simple is complex enough? *Ann Biomed Eng* 2015; 43(3): 489–500.
15. Zustiak SP and Leach JB. Hydrolytically degradable poly(ethylene glycol) hydrogel scaffolds with tunable degradation and mechanical properties. *Biomacromolecules* 2010; 11(5): 1348–1357.
16. DeForest CA and Anseth KS. Advances in bioactive hydrogels to probe and direct cell fate. *Annu Rev Chem Biomol Eng* 2012; 3(1): 421–444.
17. Lutolf MP, Lauer-Fields JL, Schmoekel HG, et al. Synthetic matrix metalloproteinase-sensitive hydrogels for the conduction of tissue regeneration: engineering cell-invasion characteristics. *Proc Natl Acad Sci U S A* 2003; 100(9): 5413–5418.
18. Clevenger TN, Hinman CR, Ashley Rubin RK, et al. Vitronectin-based, biomimetic encapsulating hydrogel scaffolds support adipogenesis of adipose stem cells. *Tissue Eng Part A* 2016; 22(7–8): 597–609.
19. Ruoslahti E and Pierschbacher MD. Arg-Gly-Asp: a versatile cell recognition signal. *Cell* 1986; 44(4): 517–518.
20. Ohga Y, Katagiri F, Takeyama K, et al. Design and activity of multifunctional fibrils using receptor-specific small peptides. *Biomaterials* 2009: 30(35): 6731–6738.
21. Melkoumian Z, Weber JL, Weber DM, et al. Synthetic peptide-acrylate surfaces for long-term self-renewal and cardiomyocyte differentiation of human embryonic stem cells. *Nat Biotechnol* 2010; 28(6): 606–610.
22. Rezania A and Healy KE. The effect of peptide surface density on mineralization of a matrix deposited by osteogenic cells. *J Biomed Mater Res* 2000; 52(4): 595–600.
23. Mann BK, Gobin AS, Tsai AT, et al. Smooth muscle cell growth in photopolymerized hydrogels with cell adhesive and proteolytically degradable domains: synthetic ECM analogs for tissue engineering. *Biomaterials* 2001; 22(22): 3045–3051.
24. Huang S and Ingber DE. The structural and mechanical complexity of cell-growth control. *Nat Cell Biol* 1999; 1(5): E131–E138.
25. Rowley JA and Mooney DJ. Alginate type and RGD density control myoblast phenotype. *J Biomed Mater Res* 2002; 60(2): 217–223.
26. Ingber DE and Folkman J. Mechanochemical switching between growth and differentiation during fibroblast growth factor-stimulated angiogenesis in vitro: role of extracellular matrix. *J Cell Biol* 1989; 109(1): 317–330.
27. Hersel U, Dahmen C and Kessler H. RGD modified polymers: biomaterials for stimulated cell adhesion and beyond. *Biomaterials* 2003; 24(24): 4385–4415.
28. Chavey C, Mari B, Monthouel MN, et al. Matrix metalloproteinases are differentially expressed in adipose tissue during obesity and modulate adipocyte differentiation. *J Biol Chem* 2003; 278(14): 11888–11896.
29. Lijnen HR, Van Hoef B, Rodriguez JA, et al. Stromelysin-2 (MMP-10) deficiency does not affect adipose tissue formation in a mouse model of nutritionally induced obesity. *Biochem Biophys Res Commun* 2009; 389(2): 378–381.
30. Niedzwiecki L, Teahan J, Harrison RK, et al. Substrate specificity of the human matrix metalloproteinase stromelysin and the development of continuous fluorometric assays. *Biochemistry* 1992; 31(50): 12618–12623.
31. Nagase H. Substrate specificity of MMPs. In: Clendeninn NJ and Appelt K (eds) *Matrix metalloproteinase inhibitors in*

cancer therapy. New York: Springer Science+Business Media, 2001, pp. 39–66.
32. Oedayrajsingh-Varma MJ, van Ham SM, Knippenberg M, et al. Adipose tissue-derived mesenchymal stem cell yield and growth characteristics are affected by the tissue-harvesting procedure. *Cytotherapy* 2006; 8(2): 166–177.
33. Astori G, Vignati F, Bardelli S, et al. "In vitro" and multicolor phenotypic characterization of cell subpopulations identified in fresh human adipose tissue stromal vascular fraction and in the derived mesenchymal stem cells. *J Transl Med* 2007; 5(1): 55.
34. Zhu X, Shi W, Tai W, et al. The comparison of biological characteristics and multilineage differentiation of bone marrow and adipose derived mesenchymal stem cells. *Cell Tissue Res* 2012; 350(2): 277–287.
35. Bourin P, Bunnell BA, Casteilla L, et al. Stromal cells from the adipose tissue-derived stromal vascular fraction and culture expanded adipose tissue-derived stromal/stem cells: a joint statement of the International Federation for Adipose Therapeutics and Science (IFATS) and the International Society for Cellular Therapy (ISCT). *Cytotherapy* 2013; 15(6): 641–648.
36. Gasparian A, Daneshian L, Ji H, et al. Purification of high-quality RNA from synthetic polyethylene glycol-based hydrogels. *Anal Biochem* 2015; 484: 1–3.
37. Luna G, Keeley PW, Reese BE, et al. Astrocyte structural reactivity and plasticity in models of retinal detachment. *Exp Eye Res*. Epub ahead of print 6 April 2016. DOI: 10.1016/j.exer.2016.03.027.
38. Kvilekval K, Fedorov D, Obara B, et al. Bisque: a platform for bioimage analysis and management. *Bioinformatics* 2010; 26(4): 544–552.
39. Mathieu PS and Loboa EG. Cytoskeletal and focal adhesion influences on mesenchymal stem cell shape, mechanical properties, and differentiation down osteogenic, adipogenic, and chondrogenic pathways. *Tissue Eng Part B Rev* 2012; 18(6): 436–444.
40. Lutolf MP and Hubbell JA. Synthetic biomaterials as instructive extracellular microenvironments for morphogenesis in tissue engineering. *Nat Biotechnol* 2005; 23(1): 47–55.
41. Sridhar BV, Brock JL, Silver JS, et al. Development of a cellularly degradable PEG hydrogel to promote articular cartilage extracellular matrix deposition. *Adv Healthc Mater* 2015; 4(5): 702–713.
42. Parmar PA, Chow LW, St-Pierre J-P, et al. Collagen-mimetic peptide-modifiable hydrogels for articular cartilage regeneration. *Biomaterials* 2015; 54: 213–225.
43. Stevens KR, Miller JS, Blakely BL, et al. Degradable hydrogels derived from PEG-diacrylamide for hepatic tissue engineering. *J Biomed Mater Res A* 2015; 103(10): 3331–3338.
44. Zanotelli MR, Ardalani H, Zhang J, et al. Stable engineered vascular networks from human induced pluripotent stem cell-derived endothelial cells cultured in synthetic hydrogels. *Acta Biomater* 2016; 35: 32–41.
45. Hamed S, Ben-Nun O, Egozi D, et al. Treating fat grafts with human endothelial progenitor cells promotes their vascularization and improves their survival in diabetes mellitus. *Plast Reconstr Surg* 2012; 130(4): 801–811.